ChemSusChem
Research Article
doi.org/10.1002/cssc.202500468
Chemistry Europe
European Chemical Societies Publishing
www.chemsuschem.org

A High-Throughput Investigation of the Binding Specificity of Carbohydrate-Binding Modules for Synthetic and Natural Polymers

Andrew Philip Rennison, Jaime Fernandez-Macgregor, Julie Melot, Fabien Durbesson, Tobias Tandrup, Peter Westh, Renaud Vincentelli,* and Marie Sofie Møller*

Carbohydrate-binding modules (CBMs) are noncatalytic domains that enhance enzyme binding to substrates. Type A CBMs show potential for engineering plastic-degrading enzymes due to their affinity for synthetic polymers. This study presents a high-throughput screening pipeline for characterizing the affinity and specificity of type A CBMs towards the synthetic polymers polyethylene terephthalate (PET), polystyrene (PS), and polyethylene (PE), and the polysaccharides cellulose, chitin, and starch. ≈800 CBMs from the families CBM2, CBM3, CBM10, and CBM64 are expressed as green fluorescent protein (GFP)-fusion proteins and tested for binding using a modified holdup assay, which produced up to 10 000 data points per day. The screening identifies ≈150 binders for PET and PE, around 250 for PS, and demonstrates family-specific binding patterns for avicel, chitin, and starch. To demonstrate practical utility, four CBMs with high PET affinity are fused to the PET hydrolase LCC^{ICCG}, enhancing activity on PET powder by around 5-fold. These CBM-enzyme fusions mitigate competitive binding to plastic impurities, improving performance in mixed plastic assays. This work significantly expands the repertoire of CBMs binding to synthetic polymers, advances our understanding of CBM-substrate interactions, and provides knowledge for engineering enzymes to tackle plastic pollution, particularly where mixed plastics pose significant challenges.

1. Introduction

Plastic pollution is a prominent environmental issue, driven by the rise in single-use plastics and inadequate disposal systems. This has led to widespread plastic dispersal in the biosphere,[1] causing numerous adverse effects.[2,3] The projection that the ocean will contain more plastic waste than fish by 2050[4] underscores the urgent need to address existing pollution and prevent future waste. Additionally, over 98% of plastic packaging is made from virgin fossil feedstocks, with 6% of global oil consumption going to plastic production,[4] highlighting the need for sustainable recycling practices.

Recycling plastic waste and creating a closed-loop economy are often proposed to mitigate the environmental impact of plastics. Generally, plastic recycling can be divided into two types, chemical/physical[5] and enzymatic[6] methods. However, both have issues. Chemical/physical methods are energetically expensive or use polluting reagents like methanol,[7] often reducing the quality of recycled polymers.[8] Enzymatic recycling, though much less developed, is currently limited to polyethylene terephthalate (PET) degradation and is not yet industrialized.[9,10] Both recycling pathways require sorting mixed plastic waste into constituent polymers, adding costs and environmental impacts. Crucially, neither can reduce existing plastic waste without collection schemes. Therefore, an in situ solution is also needed to remediate plastic pollution.

Numerous studies have identified fungal, bacterial, and algae species acting on various plastics.[11] Bacterial degradation of PET has been well reported since the discovery of *Ideonella sakaiensis* in 2016, which can use PET as its sole carbon source.[12] Significant degradation of polystyrene (PS) and polyethylene (PE) by bacterial isolates has also been shown.[13,14] Many fungal isolates from polluted environments, particularly from the genus *Aspergillus*, have demonstrated activity on these plastics.[15,16] Fungi, known for their role in the turnover of recalcitrant biomass and production of industrially relevant enzymes for bioprocessing recalcitrant material, secrete enzymes like laccases, peroxidases, and cutinases that act on lignin and complex biopolymers as well as polymers such as PE, PET, and PS.[17–19] However, enzymatic degradation of PET is much more developed than other plastics. The PAZy database (www.pazy.eu), which catalogs biochemically characterized enzymes, currently lists over 100 PET hydrolases, two nonspecific oxidase classes of PE degraders, and no enzymes for PS degradation.[20]

A. P. Rennison, T. Tandrup, P. Westh, M. S. Møller
Department of Biotechnology and Biomedicine
The Technical University of Denmark
Søltofts Plads, Building 221, DK-2800 Kgs. Lyngby, Denmark
E-mail: msmo@dtu.dk

J. Fernandez-Macgregor, J. Melot, F. Durbesson, R. Vincentelli
Laboratory Architecture et Fonction des Macromolecules Biologiques
Aix-Marseille University
Luminy Campus, 13288 Marseille, France
E-mail: renaud.vincentelli@univ-amu.fr

Supporting information for this article is available on the WWW under https://doi.org/10.1002/cssc.202500468

In nature, many enzymes involved in bioprocessing natural polymers are modular proteins, including carbohydrate-binding modules (CBMs) besides the catalytic domain. These noncatalytic CBMs can enhance enzyme activity by increasing affinity or enzyme concentration at the substrate. They can also increase enzyme specificity by directing it to a particular polymer within a complex polysaccharide environment such as the plant cell wall.[21] Several CBMs that bind to plastics have been identified,[22–24] and studies have shown their potential in engineering plastic-degrading enzymes, primarily focusing on PET degradation;[25–27] however, there are also examples of CBM fused laccases and lytic polysaccharide monooxygenases with activity on other plastics.[28,29] These CBMs are classified as type A, characterized by a planar binding surface that allows them to bind to insoluble targets,[21] and are mainly grouped into CBM families 2 and 3 (CBM2 and CBM3) in the carbohydrate-active enzymes (CAZy) database (www.cazy.org).[30] A number of other binding modules have also been identified that increase the activity of PET hydrolases when used as part of fusion enzymes, in particular PHA binding domains.[31]

While industrial scale enzymatic degradation of pure PET streams may not require a CBM,[24] municipal solid waste often comprises mixed plastics like PET, PS, and PE.[32] Enzyme cocktails for degrading mixed plastics will likely need substrate-binding domains with specificity for each plastic substrate, to avoid non-target binding. Engineering fungal or bacterial strains for in situ biodegradation of plastic pollution may also require binding domains, due to the lower substrate concentration compared to industrial conditions. Substrate-binding domains that do not bind to environmentally abundant polysaccharides like cellulose or starch would be beneficial in these conditions.

The binding of CBMs to polysaccharides and their impact on enzymatic activity have been studied for decades.[33] However, many studies have been biased towards polysaccharides that the associated catalytic domains act upon, and systematic studies testing CBMs against various polysaccharides are rare. Some studies screen multiple CBMs from different families on one substrate or test various substrates with CBMs from one family.[34,35] These limited studies do not provide sufficient data to predict binding affinity and selectivity based on sequence, structure, or phylogeny. It has been proposed that the specificity of type A CBMs is influenced by the spacing between aromatic residues in the binding plane or their relative angles.[36,37] However, these proposals are often based on testing of individual modules and may not apply across the entire family. Many type A CBM families bind both cellulose and chitin, with a distinction often made between these and starch-binding domains (SBDs). Given the similarity between the surfaces of starch granules and crystalline cellulose,[38,39] some promiscuity in binding could be expected. Understanding CBM specificity for these highly abundant polysaccharides would not only aid in developing enzymes for bioremediation of plastic waste but also enhance our knowledge of biomass turnover on Earth.

In this study, we developed a high-throughput (HTP) screening pipeline (**Figure 1**a) for type A CBMs binding to synthetic polymers (PET, PS, and low-density polyethylene, LDPE) and polysaccharides (cellulose, β-chitin, and starch). Approximately 1200 proteins from CBM families 2, 3, 10, and 64 were rationally selected, designed as fusions with an enhanced green fluorescent protein (EGFP), and expressed and purified in an HTP manner. These proteins were analyzed using an adapted holdup (HU) assay[40,41] (Figure 1b), with binding intensities (BI) calculated for each substrate (Figure 1c). CBMs that specifically bound to a given plastic were then fused to the PET-degrading enzyme LCC^{ICCG}[55,66] and the selectivity of these fusion enzymes was determined in mixed substrate assays.

2. Results and Discussion

2.1. Design of a High Throughput Assay for CBM Interactions

Inspired by a HTP holdup assay developed for identifying protein binding to peptides immobilized on insoluble beads,[40] a holdup assay to screen for proteins binding to insoluble polymers was developed (Figure 1). The protocol is almost fully automated on a Tecan liquid handling robot, using a modification of the program described previously.[41] In short, substrates were suspended in liquid and transferred to 384-well filter plates with one well out of every four remaining empty to act as a control. Following washing, EGFP-labelled CBMs were added to both the substrate and control wells and allowed to equilibrate. The liquid from each well was then aspirated into a receiver plate, and unbound protein was detected by GFP fluorescence. This enabled calculation of the BI, representing the percentage of bound protein at a single concentration relative to the control. The use of insoluble polymers, unlike the peptide-coated beads used in the original method, necessitated additional controls and considerations to ensure data quality.

To ensure accurate pipetting of the suspended substrate into the 384-well filter plates, the mass of the remaining substrate in the suspensions after the plates had been filled was checked by drying the suspension at 105 °C overnight. The consistent concentration before and after dispensing confirmed pipetting accuracy. Visual inspection verified the filling of wells, although consistency in substrate amounts per well could not be confirmed. Furthermore, the red fluorescent signal from mCherry, doped into each purified EGFP-CBM protein, served as a control to verify consistent protein pipetting and complete liquid transfer from the holdup assay to the receiver plate during centrifugation (Figure 1). False positives could arise if test wells contained less volume than the control well within a group of four. To mitigate this, wells with mCherry fluorescence outside 80–120% of the group median were excluded from BI calculations. If the control well (without substrate) fell outside this range, the entire group was excluded. Finally, a large excess of substrate relative to protein minimized the impact of volume discrepancies on binding. Overfilling had no effect, while underfilling would only result in tolerable false negatives in this HTP study.

Given that many proteins, including the fusion partner EGFP, bind nonspecifically to synthetic polymers,[42] standalone EGFP modules were randomly distributed across plates to determine

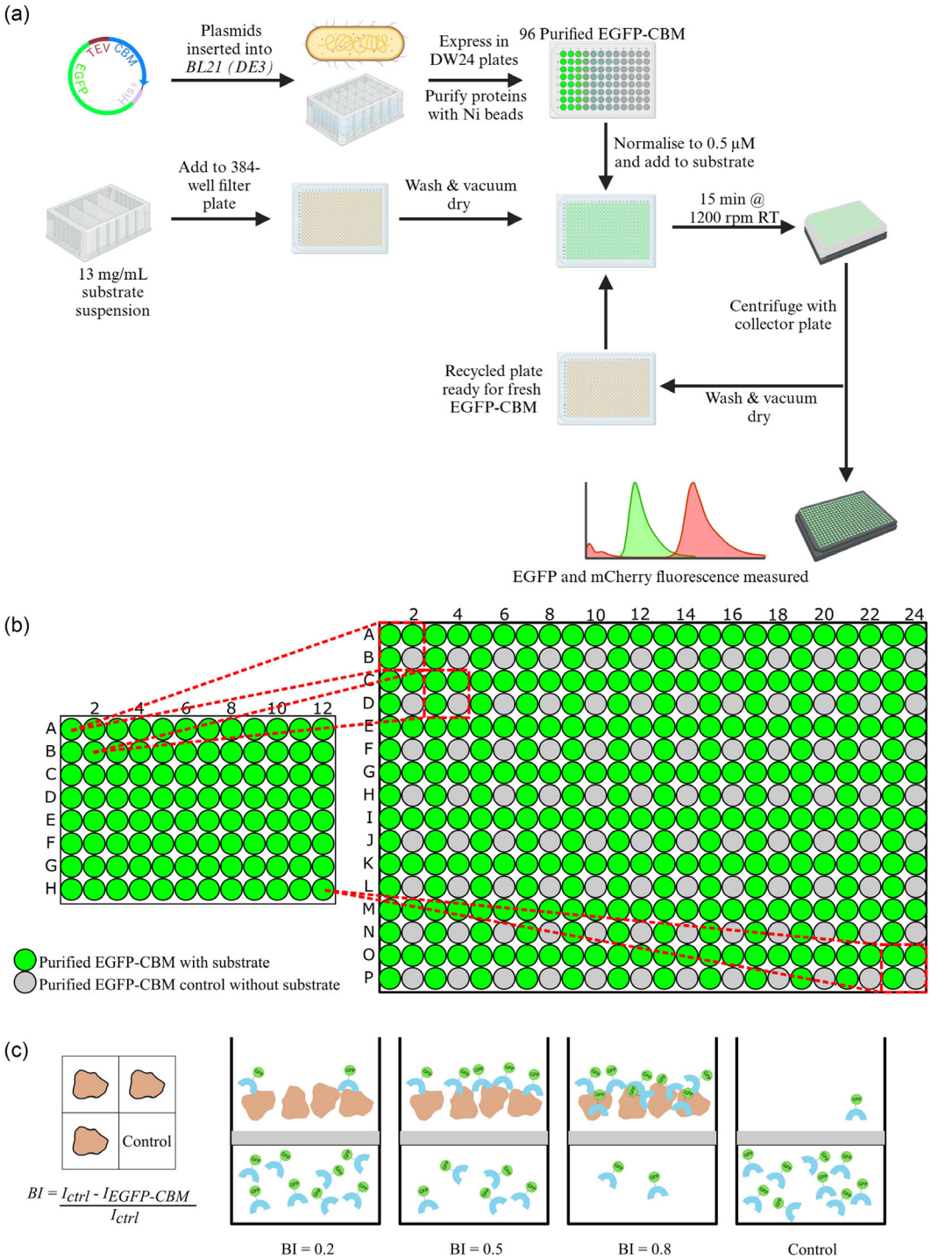

Figure 1. Setup for the high throughput (HTP) holdup assay. a) The process flow of HTP expression, purification, and binding analysis by the holdup assay. b) The setup of the 384-well filter plates used in the assays. The purified EGFP-CBM is added from the 96 well plate, to the 384 well plate in the pattern shown. The bottom right well of each group of four has no substrate added and is used as the control well. c) The conceptual framework of the holdup assay. Substrate is added to the top of the filter plate, followed by the protein, which binds to the substrate at varying levels. Unbound protein is then removed by centrifugation and collected in a 384 black plate; it is detected by the fluorescent signal from the EGFP module. BI values are calculated as a fraction of the bound total, compared to the control wells.

the mean BI of the reporter molecule on the reused substrates. EGFP showed low binding to all substrates, with PS showing the highest BI (0.14) and starch the lowest (0.09). EGFP BI values on each substrate were used as thresholds to determine whether a CBM was considered a binder in the holdup assay (*SI Appendix*, Table S1, Supporting Information).

Key decisions were made to maintain the HTP nature while retaining applicability to various substrates. To minimize

substrate use, substrates in the filter plates were reused and regenerated by washing with 1 M NaCl and 2 M urea. Two variants of a chitin binding domain (ACQ50287) were distributed randomly across the chitin test plate, and the BI was monitored over 10 rounds of washing. No decrease in binding was observed over this process, with only normal variation seen between washings (Figure S1, Supporting Information). In addition, several strongly binding proteins were identified on the other substrates after up to 10 washes, suggesting recycling of these substrates is feasible. However, the washing procedure did cause xylan to form gels within the filter plates making it impossible to recycle. In such cases, or when the availability of substrate is not a factor, fresh loading of new plates for each round of CBMs to be tested could be considered. This study focused on the interaction of type A CBMs with insoluble polysaccharides. However, type B and C CBMs could also be analyzed using soluble glycans immobilized on insoluble beads.

The HTP holdup assay results were validated for 24 representatives using a pulldown assay, with small and acceptable discrepancies observed (see Supporting Information text). BI values for synthetic polymers were generally higher in the holdup assays than in the pulldown assay. This may be due to protein interactions with residual protein on the surface due to recycling in the holdup experiments. The validation confirmed the HTP holdup assay as a reliable method for identifying the binding of CBMs to insoluble polymers. Hence, the data can be used for further analysis of CBM affinity and specificity and to identify structural features that determine these properties.

Using BI as a measure of CBM binding to substrates was necessary for adapting the holdup assay to insoluble polymers. Previously, BI was used to calculate a dissociation constant (K_d) for protein binding to peptides immobilized on agarose beads.[40] However, the heterogeneous nature of the binding sites on the polymeric substrates invalidates assumptions of one-to-one binding, making the calculation of binding site density on the surface of the particles impossible and preventing K_d calculation from a single-point assay. Though it would be possible to modify the holdup assay to produce binding curves for determining binding affinity, this would reduce data point production per protein tenfold. For identifying CBMs for enzyme design, detailed calculation of the binding parameters K_d and B_{max} was secondary to analyzing a large number of CBMs, allowing the selection of the binders and ranking the relative ability of each member of a large family of enzymes. The holdup assay could produce up to 10 000 data points per day, allowing BI calculation of ≈2500 proteins on one substrate daily, outperforming previous HTP screening techniques that measure binding on a few hundred samples per day at most.[43]

It should be noted that there are potential limitations and pitfalls associated with the holdup method as applied in this study, which warrant discussion. First, the HTP expression of the EGFP-CBM constructs was done in a standard *E. coli* BL21 expression strain for ease of use and downstream purification. However, this may have affected the number of obtained CBMs. In particular, proteins stabilized by disulfide bonds would be better expressed in specialized strains.[44] While the vast majority of CBMs selected for expression in this study were of bacterial origin, future studies involving fungal proteins may benefit from alternative expression systems, such as *Pichia pastoris*. Second, the holdup method relies on the free movement of unbound proteins through the filters, to be detected in the receiver plate. During method development for polysaccharides, it was observed that the filters became clogged with certain substrates, in particular xylan, which makes the assessment of CBM binding impossible in these cases. Additionally, large aggregates of EGFP-CBM proteins may hinder movement of unbound protein through the filter, potentially leading to false positives. However, the use of the same protein aliquots in the control wells is expected to mitigate this issue.

2.2. HTP Holdup Assays to Identify Binding Profiles of CBMs

The results and discussion of the selection and expression of the EGFP-CBM proteins can be found in the supporting information. Out of the 1097 EGFP-CBM proteins initially selected for expression, 797 yielded concentrations above 0.5 μM after purification, making them suitable for the HTP holdup assays. Details on the design and validation of the holdup assay can be found in Supporting Information text. BI values were determined for each CBM against the polymers PET, PS, and LDPE, as well as the polysaccharides avicel, β-chitin, and starch. Constructs with BI values below that of EGFP alone (Table S1, Supporting Information) on a given substrate were considered nonbinders.

Histograms depicting the binding intensities for all binders on each substrate are shown in **Figure 2**, with BI values available in *Dataset S1*, Supporting Information. The holdup assay identified 727 CBMs that bound to at least one of the six substrates, equating to a 91.2% hit rate. The raw data and results plotted for each of the 384-well filter plates are provided in *Dataset S2*, Supporting Information.

A high number of binders were observed for avicel and chitin with 432 and 412 binders, respectively. These polysaccharides also exhibited higher average BI values than the other substrates, consistent with CBM2 and CBM3 being identified as cellulose and chitin binders.[45–47] The CBMs that bound most tightly to avicel and chitin were from organisms found in environments rich in these polysaccharides, including soil bacteria, cellulose-degrading sludge communities, and plant pathogens. Both gram-positive and gram-negative bacteria and eukaryotes were represented, with CBMs from marine bacteria being among the strongest chitin binders. Previous studies have identified CBMs with comparable affinities for both cellulose and chitin,[48,49] demonstrated here by 270 CBMs binding to both substrates. Over 100 domains were identified as specific binders to either avicel or chitin, mostly within the CBM2 and CBM3 families. However, specific chitin binders all had lower BI values compared to specific avicel binders. Unsurprisingly, significantly fewer starch-binding domains were identified, with 249 in total, many of which bound weakly (Figure 2). Only 17 CBMs had a BI value on starch over 0.3, with only one approaching 0.5, a CBM2 from the bacteria *Phytohabitans suffuscus*, isolated from orchid roots. However, a much higher proportion of CBM10 and CBM64 bound to starch compared to avicel and chitin, with many of these coming from putative cellulases or xylanases.

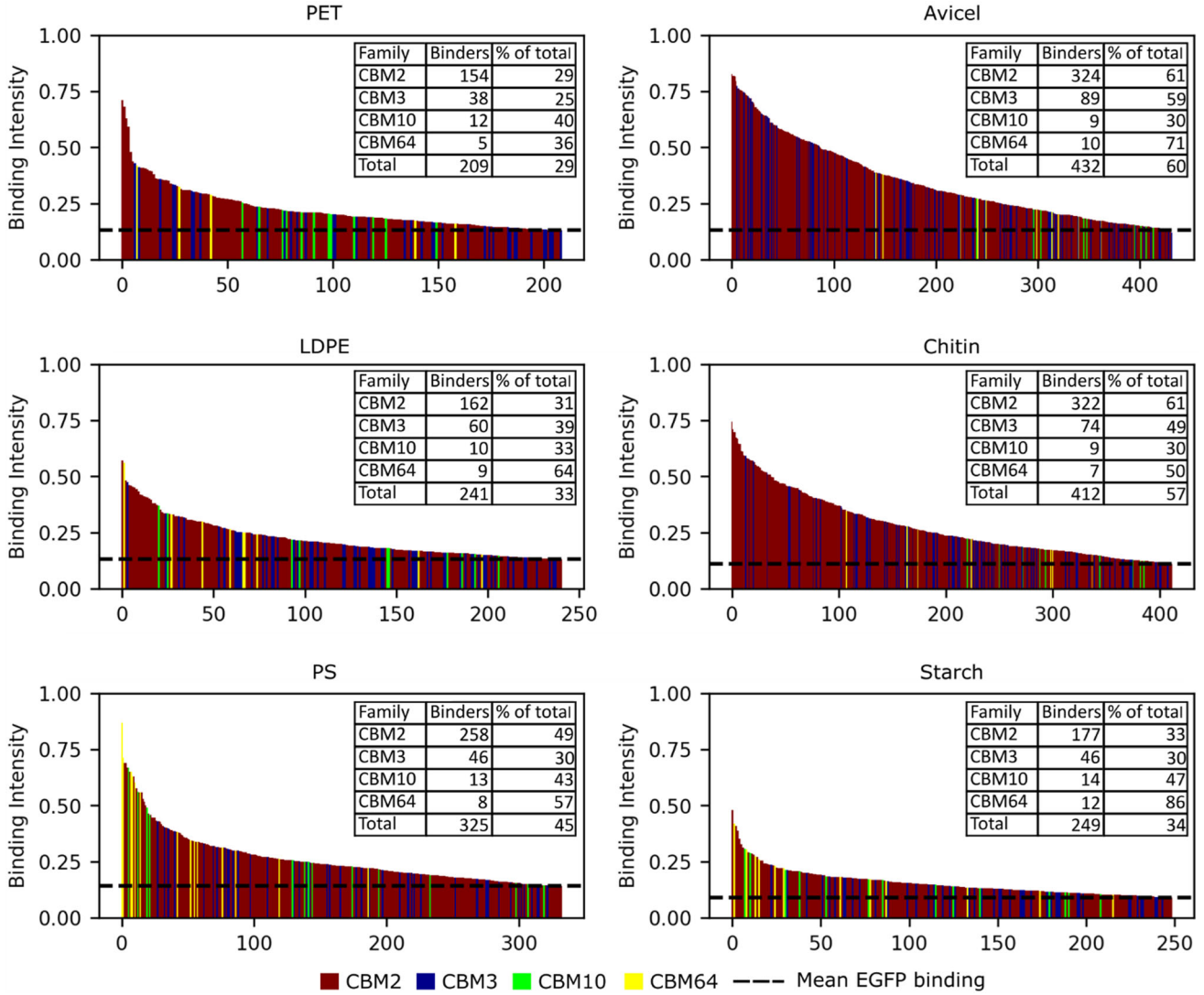

Figure 2. Histograms showing the binding intensities of EGFP-CBM constructs to each of the six substrates analyzed. Binders are identified as having a higher BI than the average of lone EGFP binding over the course of several plates, as represented by the dotted line on each histogram. The number of binders from each family and total binders on each particular substrate are seen in the insert on each plot, along with the proportion of confirmed binders from the total tested in that family. Tables of the full dataset of the proteins binding to each of the substrates can be found in Dataset S1 and S2, Supporting Information.

The most promising PET binders were found in the CBM2 and CBM3 families (Figure 2 and *Dataset S1*, Supporting Information). The highest BI on PET was 0.71 for a CBM2 from *Streptomyces bingchenggensis*, which also bound strongly to PS and avicel. Another notable protein, a CBM2 from *Rivularia sp.*, had a BI of 0.59 on PET but did not bind to the other two plastics. These BI values are significantly higher than the 0.19 measured for the widely studied PET hydrolase PHL7 (*Dataset S1*, Supporting Information). However, it should be noted that tighter binding is not necessarily advantageous for interfacial catalysis, in accordance with the Sabatier principle.[50] Therefore, a full assessment of the optimum affinity should be conducted for PET hydrolases prior to design of fusion enzymes. BI values of CBMs binding to LDPE were overall slightly lower than those for PET and PS (Figure 2 and *Dataset S1*, Supporting Information). However, notable examples of high BI values and specific CBMs were identified, including a CBM64 from the bacterium *Fulvivigra maritima*. It demonstrated specific binding to LDPE with a BI of 0.56, with several CBM2 domains also exhibiting specific binding to LDPE. Among the tested synthetic polymers, the largest number of hits were on PS, with CBM64 domains representing most of the higher BI values (Figure 2). BI values on PS were generally higher, with 20 proteins having BI values of 0.5 or greater, compared to 5 for PET and 8 for LDPE. The strongest PS binders were a CBM64 from *Spirochaeta thermophila* and a CBM2 from *Micromonosporaceae* bacterium DSM 106 523, both displaying negligible binding to PET and LDPE. The CBM10 family had similar number of hits as CBM64 but generally lower BI values (Figure 2). Notably, three CBM10s bound tightly and specifically to PS (AAA26710, AAO31760, and BAA25188|330-363).

2.3. Binding Specificity of CBMs Is Phylogenetically and Structurally Determined

The holdup assay clearly demonstrated a significant degree of specificity, with many CBMs binding selectively to one or another of the substrates. When considering only proteins that bind to a single substrate, we see over 50 candidates on each of the six substrates, with many more binding to two substrates. This diversity makes it challenging to isolate specific features of the proteins responsible for substrate-specific binding. To explore potential patterns, phylogenetic trees were constructed to assess specificity from an evolutionary viewpoint. For the polysaccharides (**Figure 3**), the trees reveal groupings of BI on individual substrates, providing some limited evidence for specificity. In contrast but not unexpected, for the plastics (Figure S2, Supporting Information), the relationship between phylogeny and specificity is less pronounced, though groupings by substrate are still apparent. It is reasonable to assume that specific structural features promote substrate-specific binding for both plastics and polysaccharides. Some of these features are outlined in the following paragraphs. While it is not intended to be an exhaustive or definitive list, if offers useful indicators for future analyses of this extensive dataset.

Phylogenetic trees were constructed with sequences of CBMs that demonstrated binding to at least one of the six substrates analyzed. These trees were split into the four CBM families and annotated with HTP holdup assay results (Figure 3, Figure S2, Supporting Information). When focusing on the natural polymers, the trees generally reflect known trends within CBM families and reveal phylogenetically determined binding subgroupings. In the CBM2 tree, avicel and chitin binding are evenly distributed (Figure 3), consistent with known preferences in this family.[45,46] Some subgroups show avicel binding dominance, while others exhibited low binding to both avicel and chitin (Figure 3a), suggesting specificity for other polysaccharides like xylan. The CBM3 tree shows a subgroup with pronounced avicel binding (Figure 3b), indicating phylogenetically determined specificity. As stated previously, the CBM10 and CBM64 families (Figure 3c,d) show stronger and more frequent binding to starch compared to the other two families, as highlighted in comparison of the trees (Figure 3).

Following the observations from the phylogenetic trees, comparisons of Alphafold2 models of selected CBMs were conducted (Figure S3–S11, Supporting Information) to identify structural specificity determinants, with a focus on the binding surface.[22] There were several examples of CBM2 that were missing the canonical aromatic triad (e.g., ADJ46832, ACY9890, and ADJ46833) but showed some substrate preference for chitin and PS, with negligible binding to the other substrates. In particular, polar or charged side chains seem to promote chitin binding in the absence of aromatic residues on the binding surface (Figure S3 and S4, Supporting Information). A significantly modified binding surface is seen in around 10 CBM2, having only a single canonical aromatic residue and a protruding loop of two or three residues containing a tyrosine orthogonal to the plane, with plddt above 95 (Figure S5, Supporting Information). These proteins did not bind any substrates significantly, except for one (AGM06248), which bound tightly to PS and chitin, potentially due to a histidine also protruding orthogonal to the surface plane. An arginine three residues after the first of the canonical binders is seen in around 10 CBM2, serving to rotate the aromatic side chain through 90°,[37] which also disrupts binding to PET (Figure S6, Supporting Information).

A majority of CBM3 modules have loop truncations removing one of the aromatic residues from the binding surface, relative to the canonical CBM3 structure (PDB: 1NBC) (e.g., ADZ85343, ABX41011, and ADZ85351). These proteins show consistently strong avicel binding (Figure S7, Supporting Information), in contrast to previous findings.[51] The subgroup with the extended loop is underrepresented among both PET and chitin binders. Around 10 of these proteins also contain a short α-helix found just after the binding residue on the fourth β-strand, which protrudes into the binding surface (Figure S8, Supporting Information). This CBM3 subgroup generally showed very weak binding to the polysaccharides, especially when the helix contained a polar residue making up the binding surface. However, two members of the subgroup, which had two hydrophobic residues in the helix contributing to the binding surface, showed moderate avicel binding, while only binding weakly to chitin.

Three of the 17 screened CBM64 members show major structural variation with an extended loop, which adds another tryptophan residue to the binding surface (Figure S9, Supporting Information). Proteins with this third tryptophan did not bind PET or LDPE significantly, but two of them bound tightly to PS. This subgroup also contains one of the modules with the highest BI on starch, with CBM64 binding starch more frequently than the other CBM families.

The HTP holdup assay identified several hundred CBMs binding to each of the six substrates tested, many of which were previously unidentified. Within the polysaccharides, the preference for starch binding by CBM10 and CBM64 indicates a previously unidentified binding tendency in these families, suggesting evolutionary development of starch binding or a lack of pressure for substrate specificity, resulting in promiscuity. A study on the CBM64 from *Spirochaeta thermophila* (ADN02703.1) showed that this CBM displays properties of both type A and B binding modes, binding to solubilized polysaccharides as well as insoluble flat surfaces.[34] This dual binding mode may explain the binding of this and other CBM64 modules to starch, with many amylopectin branches behaving as semi-solubilized polysaccharides on the granule surface.[38,39] The CBMs from each family identified in this study binding to starch all had hydrophobic surfaces extending from the canonical binding surface (Figure S12, Supporting Information), which may facilitate this dual binding as glycans extending from the starch surface wrap around the CBM during binding. Importantly, none of these CBMs originate from starch-active enzymes, so the ability to bind starch could serve as an anchor during degradation of nearby cell material.

Within the CBM2 family, a known dimorphism exists between glycine and arginine residues three positions after the first of the three canonical binding aromatic residues, with arginine rotating it through 90° and affecting the planar binding surface (Figure S6, Supporting Information). This rotation has been proposed to reduce binding to cellulose and drive specificity to xylan,[37] which was not included in the screen. Of the eleven proteins with

Research Article
doi.org/10.1002/cssc.202500468
Chemistry Europe
European Chemical Societies Publishing

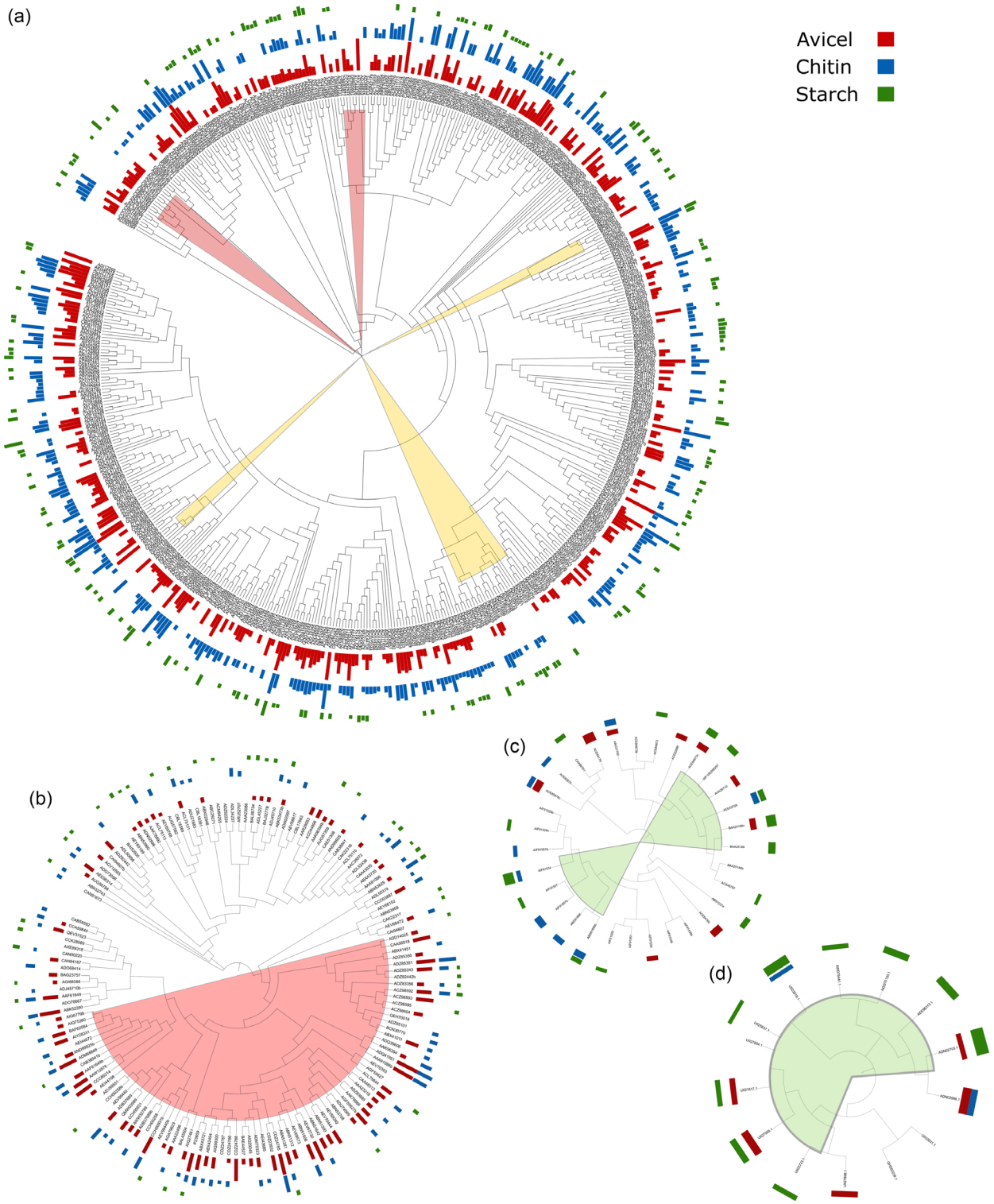

Figure 3. Phylogenetic trees including proteins with at least one confirmed binder in the holdup assays, decorated with the BI of the three polysaccharide substrates, avicel (red), chitin (blue), and starch (green). a) CBM2, b) CBM3, c) CBM10, and d) CBM64. Shading refers to groupings of proteins that bind specifically to the substrate represented by that color, with the yellow shading representing CBMs that do not bind of any of the substrates. Phylogenetic trees of the same families, decorated with the BI values of the three plastic substrates can be seen in Figure S2, Supporting Information.

arginine at this position, binding to PET and LDPE was significantly reduced, while several bound tightly to PS. Several other indicators of specificity to PS binding were observed, such as an extra aromatic binding residue in CBM64 or a tyrosine protruding from the binding surface in CBM2, with each of these possibly driven by the nonplanar conformation of aromatic rings. Each of these is a target for producing CBM variants with a high specific affinity to PS over other plastics. Most CBM2 modules have the

canonical aromatic triad of three tryptophan residues, with most of the strongest binders to each substrate represented in this group. The third position varies, featuring aromatic, polar, or aliphatic side chains. Most CBM2s with glycine in this position show negligible binding to the polysaccharides (Figure S10, Supporting Information), while histidine and serine (Figure S11, Supporting Information) allow strong binding and specificity, indicating a target for future engineering of CBM2.

Specific binding to chitin by some CBM2 members seems to be driven by polar residues either in place of or surrounding the aromatic binding residues. The presence of polar amide groups on the chitin chain would be more available for hydrogen bonding than the hydroxyl groups in cellulose, which would favor polar interactions in bonding. The CAZy database only reports one instance of CBM3 binding to chitin;[52] however, around 70 were identified here, with several showing a strong preference over avicel. Many of the CBM10 domains screened are natively found as part of repeat tandems, which do not always have the same specificity or affinity,[35] with similar effects seen in this study. Two CBM10 domains of a mannanase from *Vibrio sp.* (BAA25188) were screened alone and in their native conformation as a tandem protein, with only the C-terminal domain showing affinity for starch and avicel.

The electrostatics and hydrophobicity of the CBM surfaces were mapped to determine any associations between these and substrate specificity. Maps displaying the electrostatic potential and Wimley–White hydrophobicity[53] of each of the 1190 CBMs selected for the screen in this study can be found in *Dataset S3*. Each of the CBMs with a BI of 0.30 or more on starch showed an extended hydrophobic surface (Figure S12, Supporting Information), extending away from the canonical binding surface. In terms of the synthetic polymers, some parallels exist between the hydrophobic surfaces of the most tightly binding CBMs on each plastic (Figure S13, Supporting Information). The strongest PS and PET binders seem to have a discontinuous hydrophobic binding surface, with polar patches surrounding it. LDPE binders seem to have a more continuous hydrophobic surface, with CBM2 binding to LDPE possessing a neutral or minimally charged binding surface (Figure S14, Supporting Information). The hydrophobic and electrostatic maps also suggested further drivers of specificity between the plastics. The strongest PET binders had hydrophobic patches that were more separated compared to the PS binders, with LDPE binders exhibiting a more continuous hydrophobic surface (Figure S13 and S14, Supporting Information). Binding specificity is often influenced by the distance between aromatic residues in nature.[36] In PET binders, the separated hydrophobic patches could align with the more widely spaced aromatic moieties, as compared to PS, facilitating specificity.

2.4. CBMs can be Used to Engineer Specific Plastic Degrading Enzymes

In this study, one CBM from each of the four screened CBM families, with varying specificity to PET or PS (Table S2, Supporting Information), was fused with the commonly studied PET hydrolase, LCC^{ICCG}.[54] A linker derived from *Trichoderma reesei* Cel7A, previously used as a linker for PET hydrolase-CBM fusions,[24] was used to attach each of the CBMs to the C-terminal of the catalytic domain. The activity of these fusion enzymes on crystalline PET powder was assayed and compared to LCC^{ICCG} alone (**Figure 4**). Assays were performed at 50 °C, which is below the optimum temperature of LCC^{ICCG}, to accommodate the lower thermostability of the binding modules (Figure S15, Supporting Information). To confirm proper folding of the CBMs in the fusion enzymes, Langmuir binding isotherms to avicel were produced (Figure S16 and Table S3, Supporting Information). All enzymes, except LCC^{ICCG}-*Fl*CBM64, showed affinity for avicel not seen in LCC^{ICCG} alone. However, *Fl*CBM64 did not bind strongly to avicel in holdup and pulldown assays. Furthermore, Langmuir binding isotherms for each protein on PET and PS were also produced. LCC^{ICCG} was shown to bind nonspecifically to PET, PS, and LDPE with varying affinity. The fusion enzymes showed a range of affinities for the two substrates, with LCC^{ICCG}-*Rs*CBM2 showing the highest affinity for PET at 7.2 nM, and LCC^{ICCG}-*Fl*CBM64 the highest for PS at 8.7 nM.

CBM2s had no effect or were detrimental to activity on crystalline PET powder (Figure 4a), consistent with previous

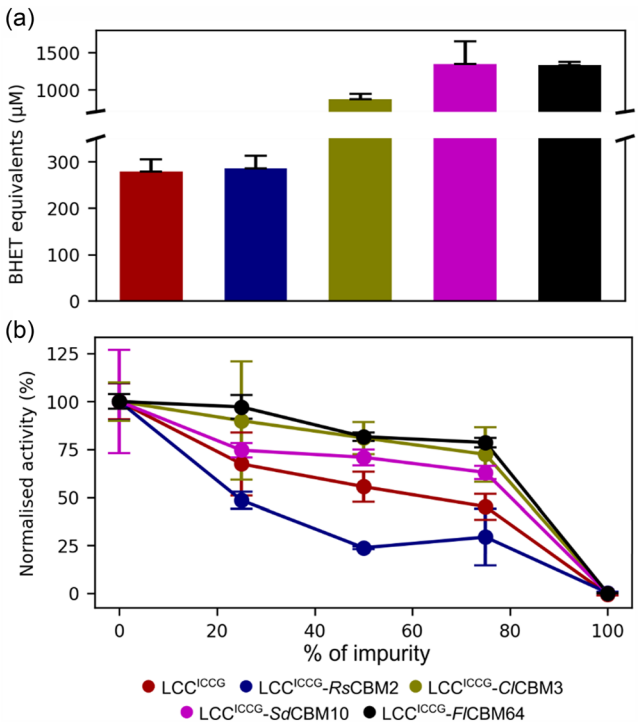

Figure 4. Activity and selectivity of fusion enzymes made with LCC^{ICCG} and CBMs obtained from the holdup assay. a) Activity of LCC^{ICCG} fusion enzymes on PET; 300 nM enzyme was incubated in 50 g L^{-1} of crystalline PET powder for 1 h at 50 °C. The concentration of degradation products was measured by UV absorbance at 240 nm and quantified using a standard curve of bis(2-hydroxyethl)-terephthalate (BHET), which serves as a representative degradation product. Each point represents the mean of triplicate experiments. b) Activity of LCC^{ICCG} fusion enzymes on PET in mixtures containing increasing amounts of PS "impurity"; 300 nM enzyme was incubated in mixtures of PET and PS for 1 h at 50 °C. The activity of the enzymes was calculated per unit mass of the PET substrate and then normalized to the activity in the experiments without impurity. Each point represents the mean of triplicate experiments.

findings.[55] However, fusions with other CBMs significantly increased PET degradation, with up to a 5-fold increase for CBM10 and CBM64 fusions (Figure 4a). It should however be stated that the % yield in each of these reactions was lower than 1% of the theoretical maximum, which is in line with previous studies on degradation of crystalline PET under these conditions.[55] To mimic a mixed plastic environment, assays were performed with increasing amounts of PS "impurity" replacing PET in the mixture to analyze the specificity of the enzymes (Figure 4b). For the fusion enzymes with *Cl*CBM3 and *Fl*CBM64, no significant reduction in activity was observed upon adding PS impurity up to 75% of the total reaction mixture, compared to a steady decrease in activity for LCC^{ICCG} alone. Conversely, the fusion enzyme with *Rs*CBM2 showed significantly lower activity on the PET substrate as the PS impurity concentration increased, indicating increased binding to the PS impurity compared to the lone catalytic domain.

The increased activity upon CBM fusion to a PET hydrolase aligns with previous studies on different PET substrates,[24] confirming that HTP screening can identify substrate-binding modules with promising applicability in enzymatic PET degradation. It should be noted that these fusion enzymes may be less applicable than LCC^{ICCG} for degrading PET in a single stream due to their lower thermal stability (Figure S15 and Table S4, Supporting Information) and the previously mentioned effects of high substrate load. However, they could offer advantages in mixed plastic environments, such as municipal solid waste.

The known PET binder *Ba*CBM2, proposed for improving PET hydrolase activity,[55] had a BI around the median for CBMs binding PET in this study. This highlights the potential of many CBMs identified here for obtaining high-affinity, high-activity PET hydrolase fusion enzymes. CBMs selectively binding LDPE and PS were also identified. To date, only two enzymes have been fully characterized with activity on PE, and little is known about their binding modes or affinity for their target, leaving scope for future design of fusion enzymes for PE degradation using the CBMs identified in this HTP screen. No enzymes in the PAZy database are currently characterized with activity on PS, but several studies have identified putative enzymes with some PS degradation capability.[56] The PS-binding CBMs identified here could aid in designing enzymes for degrading this polymer.

Strong binding of a PET hydrolase to PET does not always correlate with high activity, as dynamic adsorption and desorption are considered more relevant properties.[55] Hence, the identification of drivers of CBM affinity and specificity could facilitate the future development of CBMs tailored for engineering enzymes for specific situations. Several fusion enzymes produced in this study had enhanced activity on crystalline PET powder (Figure 4a), while also maintaining activity in the presence of another plastic, which acts as a competitor to binding (Figure 4b). Higher activity of LCC^{ICCG}-*Cl*CBM3 and LCC^{ICCG}-*Fl*CBM64 on PET alone suggests either slower adsorption or faster desorption from the PET surface, likely applying to PS as well. This would allow the enzymes to maintain higher activity on PET despite transient inactivity while bound to PS, due to increased dynamic interactions with both substrates. Development of these enzymes would be highly valuable for the enzymatic degradation of mixed plastic wastes. Furthermore, these insights could guide future engineering efforts to develop enzymes active on PS and LDPE, substrates for which enzyme discovery is ongoing.

3. Conclusion

This study presents a high-throughput methodology for systematically screening the binding specificity of type A CBMs to synthetic polymers and natural polysaccharides. Using this method, the binding of a diverse panel of CBMs from families CBM2, CBM3, CBM10, and CBM64, to three plastics (PET, LDPE, and PS) and three polysaccharides (avicel, chitin, and starch) was analyzed. This identified hundreds of binding modules with distinct substrate specificities, providing valuable insights into the structural and phylogenetic determinants behind both binding strength and specificity.

These findings highlight the potential of CBMs as modular tools for enhancing the substrate binding specificity of plastic degrading enzymes. The identification of CBMs with selective affinities for these substrates opens new avenues for enzyme engineering, allowing the design of fusion proteins tailored for improved catalytic performance in mixed plastic environments. Binding modules from family CBM3 and CBM64 were used to produce fusion enzymes with the widely studied PET hydrolase LCC^{ICCG}, which resulted in enzymes that retained activity on PET in the presence of PS as a competitive binder. Such enzymes could be valuable in the development of enzymatic recycling of mixed plastic wastes and in bioremediation.

Beyond their biotechnological applications, the observed phylogenetic and structural trends in CBM specificity contribute to a broader understanding of CBM evolution and function. The substrate preferences observed within CBM families suggest conserved mechanisms for recognizing carbohydrates within a complex environment, such as the plant cell wall. This could point to previously undescribed modes of action, such anchoring an enzyme to an inert substrate within such environments.

Overall, this study significantly expands the repertoire of characterized CBMs and establishes a foundation for leveraging these domains in biocatalytic strategies for plastic degradation. The high-throughput screening platform developed here can be further applied to explore novel CBMs on soluble and insoluble substrates, accelerating the discovery of functional binding modules for emerging biotechnological challenges.

4. Experimental Section

HTP Expression and Purification of Proteins

Expression and purification of type A CBMs fused with EGFP (see Supplementary Information for the description of the selection process) were done using a modified version of the method previously reported.[57] Expression was done in *Escherichia coli* (BL21) cells, which were grown in LB media supplemented with 50 $\mu g\ mL^{-1}$ of kanamycin. Initially, agar stabs were used to inoculate 1 mL precultures in 96-deep-well (DW) plates, which were covered with a breathable film and grown overnight at 37 °C, 200 rpm. Glycerol stocks were then made

from each culture and used for subsequent precultures. Two hundred microliters of each preculture were used to inoculate 2 mL cultures in 24-DW plates, which were grown at 37 °C, 160 rpm for 2 h before being induced with 1 μM of isopropyl-β-D-thiogalactopyranoside and grown overnight at 20 °C, 160 rpm. Cells were harvested by centrifugation at 5000 rpm and resuspended in 1 mL of lysis buffer (50 mM Tris-HCl, 500 mM NaCl, 0.1 mM phenylmethylsulfonyl fluoride (PMSF), 0.25 mg mL^{-1} lysozyme, pH 8.0) and then frozen at −20 °C. DNase I and $MgSO_4$ were added to the frozen pellets at final concentrations of 20 μg mL^{-1} and 20 mM, respectively, and the cells were lysed by thawing at 37 °C for 10 min. Next, 200 μL of 25% (dry bead volume/slurry volume) nickel chelating sepharose fast flow agarose bead slurry (Cytiva, USA) was added to the lysates, and the protein was allowed to bind with gentle shaking at 20 °C for 10 min. The lysates were then transferred to a 96-well filter plate (Machery Nagel, Germany) in a MultiScreen vacuum manifold (Sigma-Aldrich, Germany) fitted with a DW adaptor. Vacuum was applied, and the flow-through was collected in a 96-DW plate. The Ni resin beads were washed sequentially with 10 mM imidazole and 50 mM imidazole in HTP binding buffer (50 mM Tris-HCl, 500 mM NaCl, pH 8.0), and the protein was eluted in 500 μL fractions using HTP binding buffer with 500 mM imidazole. The purified protein was then stored at −20 °C prior to analysis.

HTP Screening of CBMs Against Plastics and Polysaccharides

All liquid handling for the holdup assays was performed using an Evo200 liquid handling robot (Tecan, Switzerland) with a 96-tip pipetting head. Substrates were suspended at a concentration of 13 mg mL^{-1} in either assay buffer (50 mM Tris-HCl, 500 mM NaCl, pH 8.0) or ethanol, depending on the substrate density to ensure even suspension. The settled substrate in the transfer liquid was resuspended by vigorous pipetting before transferring 75 μL to a 384-well MZHV Millipore plate with a low-binding membrane (0.45 μm Durapore PVDF membrane, Millipore, USA), delivering ≈1 mg to each well. The 384-well plates were divided into 96 groups of 4 wells in a square, with the bottom right well not containing any substrate, serving as a control (Figure 1). After substrate addition, the 384-well plates were placed on a vacuum manifold and aspirated to remove the transfer liquid. Each plate was then sequentially washed with 100 μL 1 M NaCl, 2 M urea, and assay buffer, with removal of liquid on the Tecan vacuum manifold, followed by a final wash with assay buffer and drying by centrifugation at 800 g for 5 min. Purified protein, spiked with 100 nM of an in-house produced mCherry (Uniprot: D1MPT3), was added to the 384-well filter plate, and the plate was shaken at 1200 rpm at room temperature for 15 min. The filter plate was then centrifuged at 800 g for 5 min with a 384-well receiver plate attached to the bottom. This receiver plate was then read on a PHERAstar FSX Microplate Reader (BMG Labtech) at two excitation/emission pairings: 575 nm/620 nm and 485 nm/520 nm to measure mCherry and EGFP fluorescence, respectively. After each run, the washing procedure of sequential urea, NaCl, and assay buffer washing was repeated, followed by a final wash with assay buffer and drying by centrifugation. The regenerated plate was then reused for the next cohort of EGFP-CBM constructs to be tested.

Given that only single-point concentration determinations were made during the HU assays, the K_d of the CBMs binding to each substrate could not be determined. Instead, the related parameter of binding intensity (BI) was used. This is defined in Equation (1)

$$\mathbf{BI} = \frac{I_{ctrl} - I_{substrate}}{I_{ctrl}} \quad (1)$$

where I_{ctrl} and $I_{substrate}$ refer to the intensity of the EGFP fluorescent signal in the control wells without substrate and the substrate-containing wells, respectively. The EGFP signal intensities are normalized to the median mCherry signal in a group of four wells to account for small differences in pipette volume from the 96-tip pipetting head or incomplete transfer of the liquid from the filter plate to the receiver plate during centrifugation. The BI represents the fraction of the EGFP-CBM construct bound to the substrate in the wells, allowing comparison of the relative binding strengths of the proteins at the 0.5 μM concentration used. The mean BI from each of the three wells containing substrate was reported for that particular protein on that substrate. Error bars representing the variance between the points retained after data curation are shown in the raw data and results files in *Dataset S2*, Supporting Information.

Several controls were used to ensure data quality during the HU assays. mCherry was added to every well at the same concentration, allowing for the correction of volume discrepancies by comparing its fluorescence intensity (575/620 nm band pass filter) to the median fluorescence intensity for that group. Signals not within 80–120% of the median value of the four wells were discarded and not used to determine the binding intensity. If one of the three test wells was discarded from the data analysis, either the average of two values or a single replicate was used as the reported BI. Purified EGFP protein was randomly distributed in the 96-well plates used to fill the 384-well filter plates, allowing for the determination of EGFP binding to each substrate and serving as the threshold above which a CBM was considered a binder to a particular substrate. Additionally, four known PET hydrolase enzymes, *Is*PETase, LCC^{ICCG}, PHL7, and *Tf*Cut2[12,54,58,59], were analyzed for their BI on each of the substrates as controls.

Structural Analysis of CBMs

The structure of each of the CBMs expressed in the study was modeled using AlphaFold2.[60] These models were structurally aligned using the sequence-independent and structure-based *super* algorithm in Pymol2, with 5 cycles, each having a 2.0 Å refinement cut-off for identified atom pairs. This structural alignment allowed easy comparison of 2D projections of the surface features[53,61–64] of the CBM models, including electrostatic potential and hydrophobicity, which were visualized using the SURFMAP software.[65] The electrostatic potential maps were visualized through calculation of the potential at pH 7.5. The individual 2D projections of the CBM surfaces were inspected manually.

Benchmarking HTP Binding Results Using Pulldown Assay

To benchmark the results obtained in the holdup assay, 24 of the EGFP-CBM proteins analyzed in the holdup assay were also tested using a pulldown assay. The proteins were produced and purified as described in Section 2.7. Four milligrams of each substrate in 100 μL of HTP binding buffer were added to 96-well low-binding microtiter plates, along with 100 μL of EGFP-CBM fusion protein, to a final protein concentration of 0.5 μM. Control wells without protein were also included. The plate was shaken for 15 min at 25 °C and 300 rpm in a thermomixer (Eppendorf, Germany) and then spun at 1000 rpm for 5 min in a centrifuge. Next, 150 μL of the supernatant was transferred to a new 96-well low-binding microtiter plate and centrifuged again. Then, 100 μL was transferred to a microtiter plate suitable for reading in a spectrofluorimeter. The concentration of unbound protein was determined by fluorescence using an FP-8500 Spectrofluorimeter equipped with an FMP-825 plate reader (JASCO Corporation, Japan) with excitation at 450 nm and emission at 510 nm. BI was calculated in the same way as in the holdup assay.

Langmuir Isotherms

The affinity of the proteins used in the mixed substrate assays for PET was determined by a pulldown assay. A dilution series between

10 nM and maximum 1000 nM of each protein in assay buffer was mixed with 50 mg of PET^{CP} in 300 μL volume in a nonbinding microtiter plate (In Vitro, Denmark). The samples were incubated for 1 h at 50 °C in a thermomixer (Eppendorf, Germany) and then spun at 3000 g for 5 min, and the supernatant was moved to a new plate. The amount of unbound protein was determined using a BCA assay kit (Thermofisher, USA), specifically mixing working reagent and supernatant in a 1:1 ratio followed by incubation at 37 °C for 2 h before reading absorbance at 562 nm in a spectrophotometer (Epoch Biotek, USA). The amount of bound protein in each well was calculated by subtracting the unbound from the total protein added, and the dissociation constant (K_d) was determined by fitting Equation (3) to the data.

$$[\mathbf{BP}] = \frac{[\mathbf{FP}] \cdot \boldsymbol{B}_{\max}}{\boldsymbol{K}_{\mathbf{d}} + [\mathbf{FP}]} \quad (2)$$

where [*BP*] is the coverage of protein on the substrate (nmol/g), [FP] is the concentration of unbound protein (nM), and B_{max} is the amount of proteins required to fully saturate the surface of the substrate. For the isotherms, the concentration of bound protein was expressed as nmol g^{-1}. A minimum of seven points were used to produce each binding isotherm for K_d and B_{max} determinations, and assays were run in triplicate.

PET Degradation in a Mixed Substrate Assay

Four CBMs, which demonstrated strong binding and selectivity in the holdup assay, were used to produce fusion enzymes with the PET-degrading enzyme LCC^{ICCG}.[9,10] Details of the LCC^{ICCG} fusion enzymes are provided in Table S5, Supporting Information, with sequences in Table S6, Supporting Information. They were produced and purified as described in the supplemental materials and methods. The activity of these enzymes, along with LCC^{ICCG} alone, on amorphous PET powder was assayed with increasing amounts of PS or avicel added as "impurities" to the reaction mixture. Assays were performed in 96-well low-binding microtiter plates in a 200 μL volume with an enzyme concentration of 300 nM. A total solid mass of 50 mg was maintained, with PS or avicel replacing PET with 25%, 50%, 75%, and 100% of impurity. The microtiter plates were shaken at 1000 rpm and 50 °C for 1 h and then centrifuged at 1000 rpm for 5 min. Next, 150 μL of the supernatant was transferred to a new 96-well low-binding microtiter plate and centrifuged again. Then, 100 μL was transferred to a new UV microtiter plate. The absorbance of degradation products was measured at 240 nm using a spectrophotometer (Epoch BioTek, USA), and the concentration was calculated using a standard curve. Activities were calculated and normalized to the mass of PET substrate under the specific assay conditions. These activities were then normalized to the activity of the enzyme on PET alone and plotted against the percentage of impurity in the mixture.

Additional Materials and Methods can also be found in the Supporting Information.

Acknowledgements

We would like to thank Prof. Bernard Henrissat for his invaluable help in providing sequences of the CBMs, his expert advice on the bioinformatic approaches, and his valuable feedback on the manuscript.

We would also like to thank Bo Pilgaard for his help in preparing the AlphaFold2 models of the CBMs used in this study.

We would like to thank laboratory technician trainee Sabrina Rostved for her help in the expression and purification of proteins for the pulldown assays.

This work was supported by the Danish Independent Research Council [grant number: 1032-00273B]. Furthermore, the gene synthesis work (proposal:10.46936/10.25585/60008756) conducted by the U.S. Department of Energy Joint Genome Institute (https://ror.org/04xm1d337), a DOE Office of Science User Facility, was supported by the Office of Science of the U.S. Department of Energy operated under Contract No. DE-AC02-05CH11231. The project leading to this publication has received funding from France 2030, the French Government program managed by the French National Research Agency (ANR-16-CONV-0001) and from Excellence Initiative of Aix-Marseille University - A*MIDEX. J.F.M. was funded by Consejo Nacional de Humanidades Ciencias y Tecnologias (CONAHCYT) "Becas al Extranjero Convenios GOBIERNO FRANCES 2021 - 1" grant 795494. J.F.M. recieved funding from "Espoirs de la Recherce" program managed by the French Fondation pour la Rescherche Medicale (FDT202404018637). Finally, we would like to thank the French Infrastructure for Integrated Structural Biology (FRISBI) (Grant ANR-10-INSB-05-01) for funding the equipment at AFMB.

Conflict of Interest

The authors declare no conflict of interest.

Data Availability Statement

The data that support the findings of this study are available in the supplementary material of this article.

Disclaimer Notice

This document contains results from work performed under the auspices of the U.S. Department of Energy's Office of Science, Biological and Environmental Research Program and by the University of California, Lawrence Berkeley National Laboratory, Lawrence Livermore National Laboratory and Los Alamos National Laboratory. Neither CONTRACTOR, DOE, the U.S. Government, nor any person acting on their behalf: (a) make any warranty or representation, express or implied, with respect to the information contained in this document; or (b) assume any liabilities with respect to the use of, or damages resulting from the use of any information contained in the document.

Keywords: high-throughput screening · plastic waste degradation · protein-substrate interactions

[1] C. A. Choy, B. H. Robison, T. O. Gagne, B. Erwin, E. Firl, R. U. Halden, J. A. Hamilton, K. Katija, S. E. Lisin, C. Rolsky, K. S. Van Houtan, *Sci. Rep.* **2019**, *9*, 7843.
[2] M. C. M. Blettler, K. M. Wantzen, *Water. Air. Soil Pollut.* **2019**, *230*, 174.
[3] I. A. Isangedighi, G. S. David, O. I. Obot, *Anal. Nanoplastics Microplastics Food*, CRC Press, Boca Raton, Florida, USA **2020**, 15.
[4] World Economic Forum, Ellen MacArthur Foundation and McKinsey & Company, *Ellen MacArthur Found.* **2016**, *120*, https://www.ellenmacarthurfoundation.org/the-new-plastics-economy-rethinking-the-future-of-plastics.

[5] N. Singh, D. Hui, R. Singh, I. P. S. Ahuja, L. Feo, F. Fraternali, *Compos. Part B Eng.* **2017**, *115*, 409.
[6] N. Mohanan, Z. Montazer, P. K. Sharma, D. B. Levin, *Front. Microbiol.* **2020**, *11*, 580709.
[7] J. Y. Jang, K. Sadeghi, J. Seo, *Polym. Rev.* **2022**, *62*, 860.
[8] M. Sclavons, V. Carlier, R. Legras, *Polym. Eng. Sci.* **1999**, *39*, 789.
[9] Carbios, "Our ambitions to accelerate the circularity of plastics," can be found under https://www.carbios.com/wp-content/uploads/2023/12/carbios_rdd2022_ven.pdf, **2022** (Accessed: June 2025).
[10] A. Singh, N. A. Rorrer, S. R. Nicholson, E. Erickson, J. S. DesVeaux, A. F. T. Avelino, P. Lamers, A. Bhatt, Y. Zhang, G. Avery, L. Tao, A. R. Pickford, A. C. Carpenter, J. E. McGeehan, G. T. Beckham, *Joule* **2021**, *5*, 2479.
[11] V. Tournier, S. Duquesne, F. Guillamot, H. Cramail, D. Taton, A. Marty, I. André, *Chem. Rev.* **2023**, *123*, 5612.
[12] S. Yoshida, K. Hiraga, T. Takehana, I. Taniguchi, H. Yamaji, Y. Maeda, K. Toyohara, K. Miyamoto, Y. Kimura, K. Oda, *Science 80-.* **2016**, *351*, 1196.
[13] H. S. Auta, C. U. Emenike, S. H. Fauziah, *Environ. Pollut.* **2017**, *231*, 1552.
[14] R. Mor, A. Sivan, *Biodegradation* **2008**, *19*, 851.
[15] U. Anand, S. Dey, E. Bontempi, S. Ducoli, A. D. Vethaak, A. Dey, S. Federici, *Environ. Chem. Lett.* **2023**, *21*, 1787.
[16] B. Nowak, J. Pająk, J. Karcz, B. Nowak, J. Pająk, J. Karcz, *Scannning Electron Microscopy*, IntechOpen, London **2012**.
[17] E. Butnaru, R. N. Darie-Niță, T. Zaharescu, T. Balaeș, C. Tănase, G. Hitruc, F. Doroftei, C. Vasile, *Radiat. Phys. Chem.* **2016**, *125*, 134.
[18] H. P. Austin, M. D. Allen, B. S. Donohoe, N. A. Rorrer, F. L. Kearns, R. L. Silveira, B. C. Pollard, G. Dominick, R. Duman, K. El Omari, V. Mykhaylyk, A. Wagner, W. E. Michener, A. Amore, M. S. Skaf, M. F. Crowley, A. W. Thorne, C. W. Johnson, H. L. Woodcock, J. E. McGeehan, G. T. Beckham, *Proc. Natl. Acad. Sci.* **2018**, *115*, E4350.
[19] E. Santacruz-Juárez, R. E. Buendia-Corona, R. E. Ramírez, C. Sánchez, *J. Hazard. Mater.* **2021**, *411*, 125118.
[20] P. C. F. Buchholz, G. Feuerriegel, H. Zhang, P. Perez-Garcia, L. L. Nover, J. Chow, W. R. Streit, J. Pleiss, *Proteins Struct. Funct. Bioinforma.* **2022**, *90*, 1443.
[21] H. J. Gilbert, J. P. Knox, A. B. Boraston, *Curr. Opin. Struct. Biol.* **2013**, *23*, 669.
[22] A. P. Rennison, P. Westh, M. S. Møller, *Sci. Total Environ.* **2023**, *870*, 161948.
[23] J. Weber, D. Petrović, B. Strodel, S. H. J. Smits, S. Kolkenbrock, C. Leggewie, K. E. Jaeger, *Appl. Microbiol. Biotechnol.* **2019**, *103*, 4801.
[24] R. Graham, E. Erickson, R. K. Brizendine, D. Salvachúa, W. E. Michener, Y. Li, Z. Tan, G. T. Beckham, J. E. McGeehan, A. R. Pickford, *Chem. Catal.* **2022**, *2*, 2644.
[25] D. Ribitsch, E. H. Acero, A. Przylucka, S. Zitzenbacher, A. Marold, C. Gamerith, R. Tscheließnig, A. Jungbauer, H. Rennhofer, H. Lichtenegger, H. Amenitsch, K. Bonazza, C. P. Kubicek, I. S. Druzhinina, G. M. Guebitz, *Appl. Environ. Microbiol.* **2015**, *81*, 3586.
[26] L. Dai, Y. Qu, J. W. Huang, Y. Hu, H. Hu, S. Li, C. C. Chen, R. T. Guo, *J. Biotechnol.* **2021**, *334*, 47.
[27] Y. Zhang, Z. Liu, G. Li, X. Fu, Y. Zhang, Z. Wang, Y. Tian, J. Wu, *Shengwu Gongcheng Xuebao/Chinese J. Biotechnol.* **2022**, *38*, 217.
[28] A. Munzone, M. Pujol, M. Badjoudj, M. Haon, S. Grisel, A. Magueresse, S. Durand, J. Beaugrand, J. G. Berrin, B. Bissaro, *Chem. Bio. Eng.* **2024**, *1*, 863.
[29] M. Gollan, G. Black, J. Munoz-Munoz, *BMC Biotechnol.* **2023**, *23*, 18Wor.
[30] E. Drula, M. L. Garron, S. Dogan, V. Lombard, B. Henrissat, N. Terrapon, *Nucleic Acids Res.* **2022**, *50*, D571.
[31] D. Ribitsch, A. O. Yebra, S. Zitzenbacher, J. Wu, S. Nowitsch, G. Steinkellner, K. Greimel, A. Doliska, G. Oberdorfer, C. C. Gruber, K. Gruber, H. Schwab, K. Stana-Kleinschek, E. H. Acero, G. M. Guebitz, *Biomacromolecules* **2013**, *14*, 1769.
[32] I. Janajreh, I. Adeyemi, S. Elagroudy, *Sustain. Energy Technol. Assessments* **2020**, *39*, 100684.
[33] A. B. Boraston, D. N. Bolam, H. J. Gilbert, G. J. Davies, *Biochem. J.* **2004**, *382*, 769.
[34] V. M. R. Pires, P. M. M. Pereira, J. L. A. Brás, M. Correia, V. Cardoso, P. Bule, V. D. Alves, S. Najmudin, I. Venditto, L. M. A. Ferreira, M. J. Romão, A. L. Carvalho, C. M. G. A. Fontes, D. M. Prazeres, *J. Biol. Chem.* **2017**, *292*, 4847.
[35] M. S. Møller, S. El Bouaballati, B. Henrissat, B. Svensson, *J. Biol. Chem.* **2021**, *296*, 100638.
[36] N. Georgelis, N. H. Yennawar, D. J. Cosgrove, *Proc. Natl. Acad. Sci. U. S. A.* **2012**, *109*, 14830.
[37] P. J. Simpson, H. Xie, D. N. Bolam, H. J. Gilbert, M. P. Williamson, *J. Biol. Chem.* **2000**, *275*, 41137.
[38] R. N. Waduge, S. Xu, E. Bertoft, K. Seetharaman, *Starch - Stärke* **2013**, *65*, 398.
[39] Y. Wang, Y. Tian, S. J. Christensen, A. Blennow, B. Svensson, M. S. Møller, *Food Hydrocoll.* **2024**, *146*, 109162.
[40] R. Vincentelli, K. Luck, J. Poirson, J. Polanowska, J. Abdat, M. Blémont, J. Turchetto, F. Iv, K. Ricquier, M. L. Straub, A. Forster, P. Cassonnet, J. P. Borg, Y. Jacob, M. Masson, Y. Nominé, J. Reboul, N. Wolff, S. Charbonnier, G. Travé, *Nat. Methods* **2015**, *12*, 787.
[41] G. Gogl, B. Zambo, C. Kostmann, A. Cousido-Siah, B. Morlet, F. Durbesson, L. Negroni, P. Eberling, P. Jané, Y. Nominé, A. Zeke, S. Østergaard, É. Monsellier, R. Vincentelli, G. Travé, *Nat. Commun.* **2022**, *13*, 5472.
[42] M. Goebel-Stengel, A. Stengel, Y. Taché, J. R. Reeve, *Anal. Biochem.* **2011**, *414*, 38.
[43] A. A. Salmeán, A. Guillouzo, D. Duffieux, M. Jam, M. Matard-Mann, R. Larocque, H. L. Pedersen, G. Michel, M. Czjzek, W. G. T. Willats, C. Hervé, *Sci. Reports* **2018**, *8*, 2500.
[44] A. B. Bertelsen, C. M. Hackney, C. N. Bayer, L. D. Kjelgaard, M. Rennig, B. Christensen, E. S. Sørensen, H. Safavi-Hemami, T. Wulff, L. Ellgaard, M. H. H. Nørholm, *Microb. Biotechnol.* **2021**, *14*, 2566.
[45] N. R. Gilkes, R. A. Warren, R. C. Miller, D. G. Kilburn, *J. Biol. Chem.* **1988**, *263*, 10401.
[46] T. Nakamura, S. Mine, Y. Hagihara, K. Ishikawa, T. Ikegami, K. Uegaki, *J. Mol. Biol.* **2008**, *381*, 670.
[47] E. Morag, A. Lapidot, D. Govorko, R. Lamed, M. Wilchek, E. A. Bayer, Y. Shoham, *Appl. Environ. Microbiol.* **1995**, *61*, 1980.
[48] Y. Kikkawa, M. Fukuda, T. Kimura, A. Kashiwada, K. Matsuda, M. Kanesato, M. Wada, T. Imanaka, T. Tanaka, *Biomacromolecules* **2014**, *15*, 1074.
[49] L. W. Tjoelker, L. Gosting, S. Frey, C. L. Hunter, H. Le Trong, B. Steiner, H. Brammer, P. W. Gray, *J. Biol. Chem.* **2000**, *275*, 514.
[50] J. Arnling Bååth, K. Jensen, K. Borch, P. Westh, J. Kari, *JACS Au* **2022**, *2*, 1223.
[51] O. Yaniv, G. Fichman, I. Borovok, Y. Shoham, E. A. Bayer, R. Lamed, L. J. W. Shimon, F. Frolow, *Acta Crystallogr. Sect. D Biol. Crystallogr.* **2014**, *70*, 522.
[52] S. Cai, X. Zheng, X. Dong, *J. Bacteriol.* **2011**, *193*, 5199.
[53] W. C. Wimley, S. H. White, *Nat. Struct. Biol.* **1996**, *3*, 842.
[54] V. Tournier, C. M. Topham, A. Gilles, B. David, C. Folgoas, E. Moya-Leclair, E. Kamionka, M. L. Desrousseaux, H. Texier, S. Gavalda, M. Cot, E. Guémard, M. Dalibey, J. Nomme, G. Cioci, S. Barbe, M. Chateau, I. André, S. Duquesne, A. Marty, *Nature* **2020**, *580*, 216.
[55] A. P. Rennison, A. Prestel, P. Westh, M. S. Møller, *Enzyme Microb. Technol.* **2024**, *180*, 110479.
[56] L. Hou, E. L. W. Majumder, *Materials Basel.* **2021**, *14*, 503.
[57] N. J. Saez, R. Vincentelli, *Methods Mol. Biol.* **2014**, *1091*, 33.
[58] C. Sonnendecker, J. Oeser, P. K. Richter, P. Hille, Z. Zhao, C. Fischer, H. Lippold, P. Blázquez-Sánchez, F. Engelberger, C. A. Ramírez-Sarmiento, T. Oeser, Y. Lihanova, R. Frank, H. Jahnke, S. Billig, B. Abel, N. Sträter, J. Matysik, W. Zimmermann, *ChemSusChem* **2022**, *15*, e202101062.
[59] C. Roth, R. Wei, T. Oeser, J. Then, C. Föllner, W. Zimmermann, N. Sträter, *Appl. Microbiol. Biotechnol.* **2014**, *98*, 7815.
[60] J. Jumper, R. Evans, A. Pritzel, T. Green, M. Figurnov, O. Ronneberger, K. Tunyasuvunakool, R. Bates, A. Žídek, A. Potapenko, A. Bridgland, C. Meyer, S. A. A. Kohl, A. J. Ballard, A. Cowie, B. Romera-Paredes, S. Nikolov, R. Jain, J. Adler, T. Back, S. Petersen, D. Reiman, E. Clancy, M. Zielinski, M. Steinegger, M. Pacholska, T. Berghammer, S. Bodenstein, D. Silver, O. Vinyals, A. W. Senior, K. Kavukcuoglu, P. Kohli, D. Hassabis, *Nature* **2021**, *596*, 583.
[61] E. Jurrus, D. Engel, K. Star, K. Monson, J. Brandi, L. E. Felberg, D. H. Brookes, L. Wilson, J. Chen, K. Liles, M. Chun, P. Li, D. W. Gohara, T. Dolinsky, R. Konecny, D. R. Koes, J. E. Nielsen, T. Head-Gordon, W. Geng, R. Krasny, G. W. Wei, M. J. Holst, J. A. McCammon, N. A. Baker, *Protein Sci.* **2018**, *27*, 112.
[62] J. Kyte, R. F. Doolittle, *J. Mol. Biol.* **1982**, *157*, 105.
[63] E. D. Levy, *J. Mol. Biol.* **2010**, *403*, 660.
[64] M. Mezei, *J. Mol. Graph. Model.* **2003**, *21*, 463.
[65] H. Schweke, M. H. Mucchielli, N. Chevrollier, S. Gosset, A. Lopes, *J. Chem. Inf. Model.* **2022**, *62*, 1595.
[66] S. Sulaiman, S. Yamato, E. Kanaya, J.-J. Kim, Y. Koga, K. Takano, S. Kanaya, *Appl. Environ. Microbiol.* **2012**, *78*, 1556.

Manuscript received: March 5, 2025
Revised manuscript received: June 16, 2025
Version of record online: July 14, 2025